Polish J. Chem., **76**, 857–873 (2002)

Characterization of Chromium Oxide Supported on Silica

by W.K. Jóźwiak, W. Ignaczak, D. Kincel, J. Góralski and T. Paryjczak

Institute of General and Ecological Chemistry, Technical University of Łódź,
ul. Żwirki 36, 90-924 Łódź, Poland
e-mail: wjozwiak@ck-sg.p.lodz.pl

(Received August 13th, 2001; revised manuscript March 4th, 2002)

Thermal stability and redox behavior of the surface Cr-oxo structures supported upon silica were investigated by: TPR, TPO, XRD, IR and XPS techniques. During reduction in hydrogen, the surface Cr(VI) oxide phase is completely transformed into the Cr(III) oxidation state. For low loaded Cr/SiO_2 samples almost fully reversible interconversion Cr(VI) $\leftrightarrow$ Cr(III) was found during TPR – TPO cycling up to 900°C. For higher loaded samples, temperature depended oxygen – hydrogen cycling strongly influences the relative composition of chromium oxide phase supported on silica. The coexistence of three major forms of chromium oxide phase in supported CrO_3/SiO_2 system has been confirmed: monomolecularly dispersed chromates strongly bonded to silica surface, relatively inactive stable crystallites of α-chromia and intermediate metastable amorphous aggregates of CrO_3. The relative contribution of each form strongly depends on the chromium content, method of preparation, treatment conditions (temperature, atmosphere and water traces). The anchoring of chromate-like species requires suitable support adsorption sites and their concentration is governed by hydroxyl group population. Mobile hydroxo species of CrO_3 may migrate on the silica surface, anchoring to preferable adsorption sites and forming stable chromate-like species. It was also found that water is involved in the hydrolytic process of monochromated species destabilization, resulting in partial transition Cr(VI) $\rightarrow$ Cr(III). Thermodynamically favored chromium sintering process, chromates $CrO_4^{2-} \rightarrow$ crystalline α-Cr_2O_3, requires water as destabilization agent for hydrolytic splitting of Cr – O – Si linkages and chromium oxide agglomeration.

Key words: chromium oxide species, Cr/silica oxidation, temperature-programmed reduction (TPR), IR, XPS spectroscopy

The industrial importance of silica supported chromium oxide catalysts developed by Phillips Petroleum has generated much interest in their physicochemical properties [1–5]. Chromia-based catalysts have been devoted not only to the polymerization activity, but also to other important applications, *e.g.* hydrogenation and dehydrogenation of hydrocarbons, dehydration and dehydrogenation of alcohols to produce aldehydes, ketones and alkenes, water gas shift reaction, dehydrocyclization of paraffines, and the automotive exhaust purification [6–9]. Supported chromium oxide system has recently been applied for the deep oxidation of chlorinated volatile compounds [10].

Although many chromium compounds are used as catalyst precursors (*e.g.* CrO_3, $Cr(NO_3)_3 \cdot 9H_2O$, $Cr(OH)_3$, Cr_2O_3), chromium trioxide is frequently applied for the preparation of chromia supported catalysts [11–15]. During the preparation in an oxidative atmosphere, CrO_3 is transformed on the catalyst surface into chromate-like

species CrO_4^{2-}. The required catalyst activity is acquired during the reduction of Cr-oxygen species, what is crucial for certain catalytic reactions, *e.g.* for ethylene polymerization [9]. Although the structure of the supported and the unsupported chromium oxide phases was investigated in detail, the nature of chromium oxide species remained in many cases under discussion. When chromium is supported on silica, alumina and other oxidic supports, more than one single oxidation state is observed in most cases, depending on the Cr loading, preparation procedure, and treatment conditions applied (see, *e.g.*, [16–21] and literature cited therein). In general, every oxidation state of chromium between Cr(II) and Cr(VI) was postulated or proven as surface species.

The unsupported bulk CrO_3 is not stable at higher temperature. After melting above 200°C [22] it starts to decompose, forming chromium oxides Cris not 08c(4)(624 0 06.824 429.1778)]T54854.1331 Tm0

such as: nature of support and conditions of catalyst preparation and oxidation, temperature, contacting gas and the presence of water vapor.

Low loaded 0.6–2.6% Cr/silica system was investigated by Ellison *et al*. [5] using TPR method. They have found that samples of CrO_3 supported on silica, when activated in dry air, consisted mainly of chromate-like surface species with aggregates of CrO_3 and dichromate-like surface species present in varying proportions, depending upon chromium loading, method of preparation and activation conditions. Their assignment was based on comparison with TPR profiles for bulk CrO_3, Na_2CrO_4 and $Na_2Cr_2O_7$ compounds. Such approach may be misleading, taking into account defective amorphous character of silica surface, which could result in less or more disturbed chromate-like tetrahedra linked to silica surface and finally differing in their reducibility.

In this paper the temperature programmed reduction in hydrogen was used for the elucidation of Cr/silica redox reversibility. The redox behavior plays an important role not only in activation procedure but also in other applications, such as automotive exhaust purification or high temperature combustion catalysts. To this purpose reduction-reoxidation cycles were performed for samples of different Cr content and for different reoxidation temperature. Additionally, XRD, XPS and IR spectroscopy were used to characterize the chromium oxide structures supported on silica gel.

EXPERIMENTAL

Preparation of catalysts. For the silica sol-gel preparation, as a parent substance, the tetramethoxysilane (Fluka manufacture, purity ≥98%) was used. The catalysts were prepared by incipient-wetness method, in which a high specific surface area silica (535 m^2/g, BET, pore specific volume – 0.58 cm^3/g) was impregnated with aqueous solution of CrO_3. After impregnation step, the catalysts were dried at room temperature and then samples were slowly heated at a rate of 2°C per minute from 25 to 110°C and finally held on at this temperature through 5 hours. Care was taken during this procedure, since too rapid drying may lead to chromatography of the chromic acid on support surface with subsequent heterogeneity of the samples. Applying this method samples containing 0.5, 1.25, 2.73, 5.07, 6.5 and 8.5 wt % chromium were prepared. Additionally, $CrO_3 – SiO_2$ mechanical mixture (1 wt % Cr) was prepared by dry mixing and used for comparison. Determination of the chromium content was verified by atomic absorption spectroscopy (ICP-AES).

Surface area measurements. The BET method was applied to the 77 K adsorption of nitrogen on a Carlo Erba Sorptiomatic 1900.

Thermogravimetric [TG] measurements. They were made in a Thermo-analyzer TG - DTA-SETSYS 1618 apparatus applying computed technique. Sample of 20 mg was heated from 20°C up to 1100°C with linear growth 5°C·min^{-1} in dry argon stream at a flow rate of 45 $cm^3 \cdot min^{-1}$. The amount of water adsorbed on silica surface was taken into account in the quantitative interpretation of TG curve.

Hydrogen reduction. Temperature programmed reduction (TPR) measurements were carried out with a commercial temperature-programming system, Altamira Instruments, model AMI-100 equipped with a thermal conductivity detector. As reducing agent purified gas mixture 10% H_2 – 90% Ar at the volumetric flow rate of 50 $cm^3 \cdot min^{-1}$ was used. The catalyst bed containing approximately 0.1 g sample was heated in a quartz reactor from 25 up to 900°C with linear growth of 20°C·min^{-1}. At the beginning the sample was calcined at 400°C in a stream of purified gas mixture of 10% O_2 – 90% He for two hours, followed by TPR run. Then succeeding TPR runs were carried out in a similar way by previous reoxidation (2 h) treatment of sample at: 500, 600, 700 and 900°C, respectively. The effect of reduction was determined

through comparison the area enveloped by the TPR profile with that obtained for the signal corresponding to the introduction of a known amount of hydrogen into the gas stream.

X-ray diffraction (XRD) measurements. Diffraction patterns were performed with a polycrystalline D 5000 Siemens X-ray diffractometer. It was operating with a scanning speed of 0.03° per 10 s. Diffraction patterns were recorded in the range of $2\theta = 10–90°$, using nickel – filtered CuKα radiation.

Infrared technique: FTIR diffuse reflectance measurements were carried out using FTIR Shimadzu Spectrometer. For monitoring the surface hydroxyl groups stretching region at 4000 to 3000 cm^{-1} was applied and 40 scans were averaged. Before IR analysis the samples were subjected to high temperature treatment (600°C, 2 h) in dry oxygen atmosphere.

XPS technique. XPS measurements were run on a Quantum 2000 spectrometer using a pass energy of 23.50 eV. The AlKα photons were applied to excite the photoemission. All the samples were measured as powders spread on a double-side scotch tape.

RESULTS AND DISCUSSION

Silica surface stabilizes chromium oxo species as a result of esterification reaction between chromic(VI) acid and silica surface hydroxyl groups, taking place during catalyst dehydroxylation. Higher temperature oxidation leads to molecularly dispersed chromate-type species, which are precursors for catalytically active sites.

The thermogravimetric method of measuring the hydroxyl population on silica was applied and typical TG profile are presented in Fig. 1. The analysis of this curve confirms, that physically absorbed water is completely removed from silica heated at about 200°C. Further heating up to 1100°C led to evolution of water equal 3.49 wt % of silica mass. Referring this value to surface dehydroxylation and comparing with silica surface area (535 m^2/g), the total monolayer concentration of surface hydroxyl groups on silica surface was evaluated as 4.36 OH /nm^2. This value is in a good agreement with the literature value 4–5 OH/nm^2 [33]. The decrease of silica sample weight from 200 to 1100°C, represented by TG curve **a** in Fig. 1, is assigned to dehydroxylation of the silica surface. The quantitative evaluation of this process is given in Table 1 and the dependence of the concentration of hydroxyl groups on silica surface in function of temperature is also presented as curve **b** in Fig. 1.

Table 1. The effect of temperature on silica surface hydroxyl group concentration.

Temperature [°C]	OH /nm^2
200	4.37
300	3.95
400	3.07
500	2.26
600	1.73
700	1.41
800	1.20
900	0.89
1000	0.39

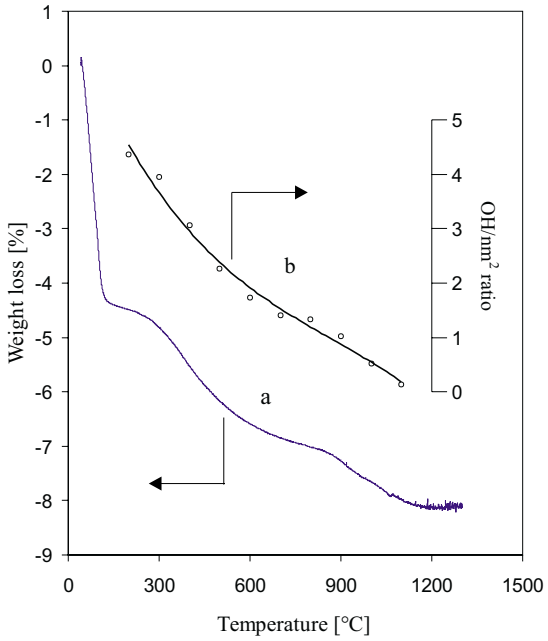

Figure 1. Results of thermogravimetric analysis for SiO_2. Curves a and b denote weight loss (%) and the OH/nm^2 ratio, respectively.

TPR studies. The examples of representative experimental TPR profiles for 1.25 wt % Cr/SiO_2 catalyst, and for 1 wt % CrO_3 – SiO_2 mechanical mixture in function of the reoxidation temperature are shown in Fig. 2 and 3, respectively. For the low chromium loading (0.5–2.73 wt % Cr) TPR profiles were characterized by a single relatively broad reduction peak with its temperature of maximum located at 465–490°C. These profiles were assigned to a single step reduction of monochromatic species, stabilized on silica surface. The increase in the reoxidation temperature led to gradual decrease of the surface area enveloped by the TPR curves, shifting the maxima to temperatures slightly higher than 500°C after final reoxidation at 900°C. Such behavior confirms the interaction of the chromate species on the support surface, induced by SiO_2, and a partial lack of full chromium redox reversibility of Cr(VI) ↔ Cr(III). The last effect is attributed to the sintering process of chromium, leading to formation of crystalline Cr_2O_3 on silica surface and confirmed by XRD method (see also Fig. 9). Crystalline α-chromia is the most stable chromium compound, highly resistant both for reduction and oxidation treatment. The TPR profiles for mechanical mixture of silica and chromium trioxide CrO_3 (1 wt % Cr) are similar to those representing the impregnated low loaded Cr/silica catalyst (compare Figs. 2 and 3). The only difference is represented by a significant decrease of the sample reducibility after reoxidation at 500°C in comparison with the first oxidation treatment at 400°C. This effect is related to a rather poor dispersion of chromium in CrO_3 – SiO_2 mechanical mixture, despite the fact that the melting of CrO_3 at about 210°C should facilitate the interface contact between CrO_3 and SiO_2.

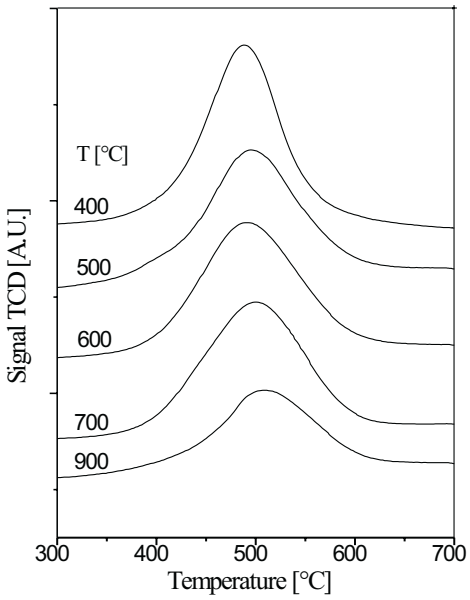

Figure 2. H_2 TPR profiles for 1.25 wt % Cr/SiO_2 catalyst after 2 h in stream of 10% O_2 – 90% Ar gas mixture, initially oxidized at 400°C, then reoxidized at 500, 600, 700 and 900°C, respectively.

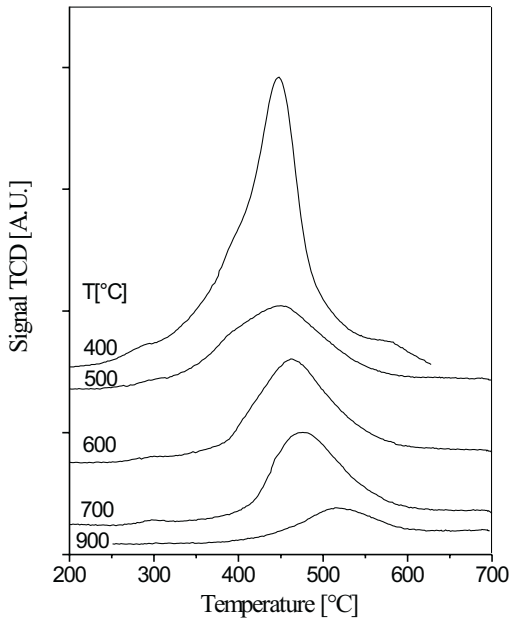

Figure 3. H_2 TPR profiles for CrO_3–SiO_2 mechanical mixture containing 1.0 wt % Cr after 2 h in stream of 10% O_2 – 90% Ar gas mixture, initially oxidized at 400°C, then reoxidized at 500, 600, 700 and 900°C, respectively.

For higher chromium loaded samples (5.07–8.5 wt % Cr), TPR profiles for samples reoxidized at different temperatures are illustrated by the representative profiles of the 5.07 wt % Cr sample in Fig. 4. The reduction profile for a fresh sample, after its oxidation at 400°C, is characterized by one reduction peak similarly like in the case of the low-loaded samples. Surface chromate like macrostructure anchored to silica seems to be responsible for this reduction effect. The H_2 uptake for this sample, being reoxidized at temperature 500°C, is represented by a rather broad TPR profile, consisted of two partly overlapped reduction peaks, attributed to the reduction of CrO_3 aggregates and surface chromates, respectively. Further increase of the reoxidation temperature led to gradual diminishing of reduction effects and simultaneously caused the relative decrease of the first peak and the growth of the second one. Using the computer aided deconvolution, the position and relative proportion of each overlapping component was estimated. The appropriate program of calculation was based on the assumption of a Gaussian peak shape and permitted the detection of individual components. For highly loaded samples two kinds of chromium species, with their maxima located at 385–400°C and 470–490°C, were assigned to aggregates of CrO_3 and chromate-like surface structures [28]. The relative proportion of the individual constituents can be calculated with an error of about 5%. Illustration of this approach is showed, for example in Figs. 5 and 6 for 5.07 and 8.5 wt % Cr/SiO_2 catalysts, respectively. Enhancement of reoxidation temperature up to 700–900°C corresponds to

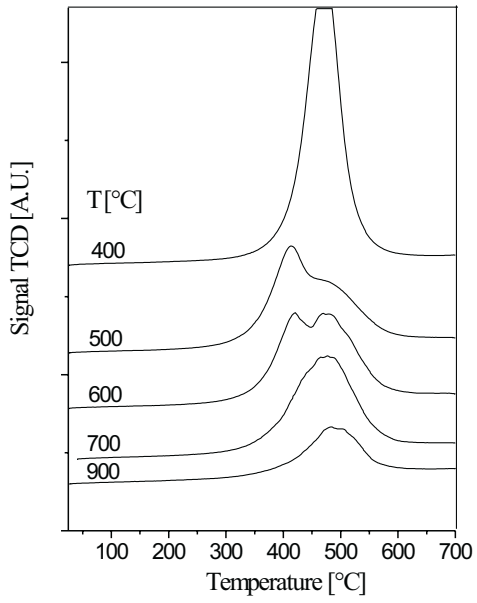

Figure 4. H_2 TPR profiles for 5.07 wt % Cr/SiO_2 catalyst after 2 h in stream of 10% O_2 – 90% Ar gas mixture, initially oxidized at 400°C, then reoxidized at 500, 600, 700 and 900°C, respectively.

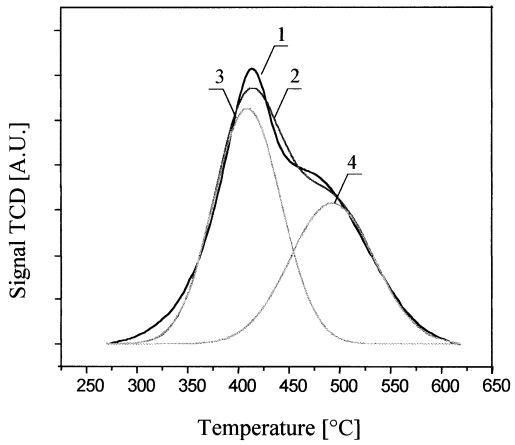

Figure 5. The deconvolution of the TPR profiles for 5.07 wt % Cr/SiO_2 sample reoxidized at 500°C for two hours. 1 – experimental profile, 2 – calculated profile, 3 and 4 – individual profiles of components.

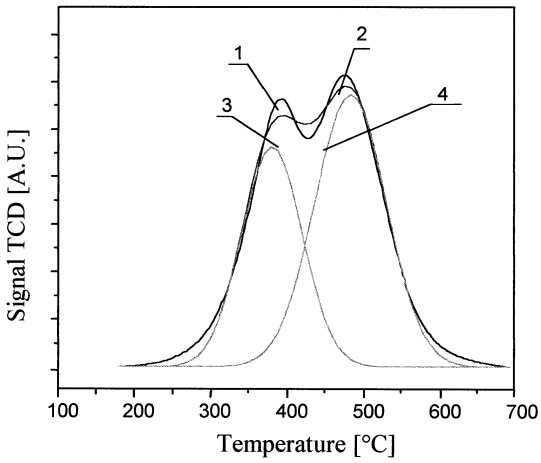

Figure 6. The deconvolution of the TPR profiles for 8.5 wt % Cr/SiO_2 reoxidized at 600°C for two hours. 1 – experimental profile, 2 – calculated profile, 3 and 4 – individual profiles of components.

the appearance of broad one peak rather independent of chromium loading. The disappearance of the low temperature constituent is assigned to the irreversible transformation of amorphous CrO_3 aggregates into crystalline Cr_2O_3, which does not participate in redox cycle [3]. The reduction degree of CrO_3/SiO_2 catalysts was evaluated on the basis of TPR profiles, such as those in Figs. 2–4, according to:

$$2CrO_3 + 3H_2 \rightarrow Cr_2O_3 + 3H_2O \quad (1)$$

The computed values depended on chromium loading and the reoxidation temperature are presented in Table 2.

Table 2. Degree of reduction for CrO_3 supported on gel-silica.

% Cr	Cr atoms $Cr_{(T)}/nm^2$	Temp. [°C]	α_1 [%]	α_2 [%]	α_s [%]	$\alpha_{exp.}$ [%]
0.5	0.0986	400–900	0	100	100	100
1.25	0.246	400–700	0	100	100	100
		900				77.7
2.73	0.538	400				98
		500				72
		600				71
		700				64.4
		900				38
5.07	0.999	400				96.2
		500	34.9	26	60.9	62.5
		600	20.5	39.9	60.4	62
		700				60.4
		900				30.1
6.5	1.28	400				94.5
		500	31.1	20.4	51.5	53.5
		600	15.9	32.3	48.2	49.4
		700				43.6
		900				16.1
8.5	1.67	400				88
		500	31.4	18.8	50.2	52.3
		600	18.6	27.1	45.7	46.9
		700				40.2
		900				15.8
1.0 mech. mix.	0.197	400				66.7
		500				27.5
		600				27.5
		700				21.5
		900				10.3

where: $Cr_{(T)}$ expresses the total quantity of chromium atoms per nm^2 of silica.
α_1, α_2 – Denote degree of reduction calculated by deconvolution of the TPR profiles for CrO_3 agglomerates and monochromate-like species.
$\alpha_s = \alpha_1 + \alpha_2$ – Total degree of reduction for CrO_3 agglomerates and monochromate-like species together.
α_{exp} – Degree of reduction for CrO_3/SiO_2 catalysts obtained experimentally.

A degree of reduction close to 100% was obtained for all CrO_3/SiO_2 catalyst samples (0.5 up to 6.5 wt % Cr) oxidized at 400°C. Only in the case of a highly loaded sample (8.5 wt % Cr) or a mechanical mixture CrO_3 – (1 wt % Cr) the degree of reduction was considerably lower than 100%. The reoxidized samples show lower degrees

of reduction, depended strongly on the temperature of reoxidation (500–900°C) and the chromium loading. In the case of low loaded samples (0.5–1.25 wt % Cr), the reduction was complete in temperature range of reoxidation 500–900°C. This proves the presence of a highly stable population of monochromate, like species on silica surface, which are involved in the reversible interconversion Cr(VI) ↔ Cr(III). The monochromate-like species are stable up to 900°C in oxidative and inert atmosphere and as Cr(III) oxo-species they are not destabilized in hydrogen.

Although the stoichiometry based on (1) is widely accepted when hydrogen is used for reduction of bulk Cr(VI) oxo compounds [3], equation (1) itself may be misleading for molecularly dispersed CrO_3/SiO_2 system, because Cr_2O_3 cannot be a reduction product of the isolated tetrahedral CrO_4^{2-} species containing two oxygen bridges with silica surface and two terminal oxygen atoms. The mechanism of such reduction, involving the removal of two terminal oxygen atoms, would result in the non modified two oxygen linkages with silica, what should lead to $Cr(II)O_2^{2-}$ species. Such unstable Cr(II) species may be expected when carbon monoxide is used as reducing agent [22,30], but in the case of water being the product of reaction with hydrogen one would rather infer the oxidation of Cr(II) to Cr(III) species. In order to explain the apparent discrepancy, we propose that the neighboring hydroxyl group may be involved in hydrogen reduction of the isolated tetrahedral CrO_4^{2-} species, according to:

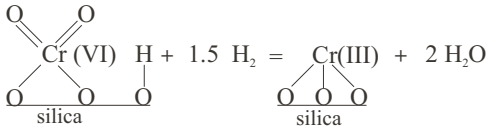

(2)

Such mechanism is in accordance with (1) and can be envisaged taking into account the expected concentration of hydroxyl groups located in the direct vicinity of the anchored chromium on silica surface (see Table 1). The Cr(III) oxo species are often regarded as the catalytic sites on silica surface in many reactions. The excessive amount of chromium (above saturation of silica surface) is inevitably transformed in the final stable form of crystalline chromia. This process is clearly visible for highly loaded chromium supported silica catalysts. More than 80% of chromium undergoes this final transformation. One can anticipate the third type of chromium oxide structure on silica surface, which is even more easily reducible than chromate-like structure and reversibly reoxidized between range 500–700°C. This agglomerated chromium oxide structure is rather amorphous and relatively weakly bonded to silica surface.

A general scheme of CrO_3 – SiO_2 system transformation may be postulated: chromate ↔ amorphous agglomerate → α-chromia on the basis of hydroxyl groups concentration on silica surface (Table 1) and the degree of reduction of CrO_3/SiO_2 catalysts (Table 2). The applied procedure of TPR curves deconvolution allows the evaluation of the different chromium structures population in function of the reoxidation temperature. Denoting the chromate type structure population as α_2 and ag-

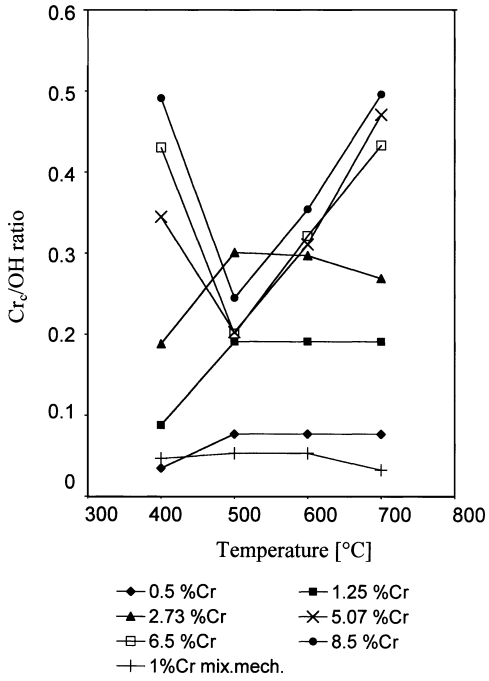

Figure 7. The calculated Cr_c/OH ratio *versus* reoxidation temperature for examined samples.

glomerate type structure as α_1 and taking into account the total chromium content Cr_T, one can calculate Cr_C value for chromate like structure on silica surface, using the amount of hydrogen consumed in TPR run according to (1). The sum of α_1 and α_2 gives α_s and represents the reducible chromium oxide population on silica surface. These values and also the total concentration of supported chromium per square nanometer of silica Cr_T are presented in Table 2. The concentration of chromate like species can be calculated using $Cr_C = \alpha_2\, Cr_T/100$. For low loaded samples (0.5–2.73 wt % Cr) when $\alpha_2 = \alpha_s = 100\%$ the almost entire chromium population is engaged in chromate like structures $Cr_T = Cr_C$. The applied procedure of TPR curves deconvolution allows for the evaluation of the different chromium structures population as a function of the reoxidation temperature. The calculated ratios between chromate like population Cr_C and hydroxyl group concentration in function of reoxidation temperature are presented in Fig. 7. As each TPR run was terminated at 700°C, the calculated Cr_C/OH ratios were based on the value 1.41 OH/nm^2 for sample reoxidation at 500, 600 and 700°C. For a fresh sample, after its first oxidation at 400°C, the value 3.07 OH/nm^2 was used (Table 1). The upper limit of chromate like monolayer on silica surface depends on hydroxyl group concentration and the theoretical value of Cr_C/OH ratio equal to 0.5 can be inferred according to:

$$CrO_3 + 2OH^- \rightarrow CrO_4^{2-} + H_2O \qquad (3)$$

The experimental value, close to monolayer coverage, was obtained for 8.5 wt % Cr/SiO_2 sample after its oxidation at 400°C (Fig. 7). A dramatically lower reducibility, observed for highly loaded Cr/SiO_2 samples after their reoxidation at 500°C, was attributed to transformation of chromate like species into amorphous and crystalline chromia phases during the first TPR run up to 700°C. The partial recovery of chromate-like species, as a result of chromium redispersion, was observed at a still higher temperature of reoxidation 600 and 700°C [3]. For low loaded Cr/SiO_2 samples up to 2.73 wt % Cr, almost the entire population of chromate like species was preserved in the redox cycling up to 700°C (Fig. 7). The above interpretation is based on the deconvolution procedure, applied for TPR profiles enabling the quantitative recognition between chromate and amorphous phases.

IR studies: The IR diffusion-reflectance spectra for 0.5, 1.25 and 2.73 wt % Cr/SiO_2 samples and silica alone after heating in stream of oxygen at 600°C for 2 h are shown in Fig. 8. These spectra represent the stretching region of SiO_2 hydroxyl groups. They show a sharp band at 3740 cm^{-1}, which has been assigned to the isolated OH groups. The partial disappearance of this band for 0.5 and 1.25 wt % chromium loading samples indicates that the chromium oxide interacts with the silica by removal of the surface hydroxyl groups simultaneously, creating a surface phase as definite compounds, which partially occupies silica surface (equation 2). The disappearance of the 3740 cm^{-1} band on account of addition of chromium oxide was already reported [27]. However, in the case of greater chromium loading 2.73 wt % Cr, one

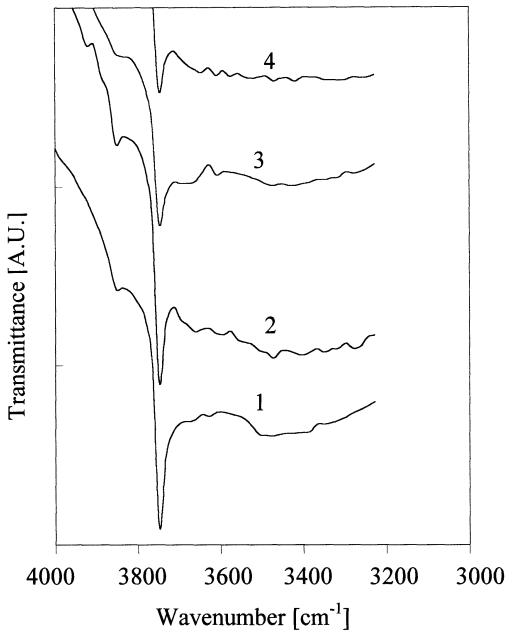

Figure 8. FTIR diffuse-reflectance spectra of hydroxyl region for silica and CrO_3/SiO_2 catalysts after temperature treatment in stream of oxygen at 650°C, 2 h. Curves: 1 – silica alone, 2, 3 and 4 for 0.5, 1.25 and 2.73 wt % chromium loading samples, respectively.

did not observe a further decrease of hydroxyl band and this observation is attributed to saturation coverage of silica surface by chromate like species formed during oxidation at 600°C. The presence of OH group population on silica, even for highly loaded chromium catalysts, may be proposed as a source of hydrogen involved in the very beginning step of ethylene initiation on Cr/silica surface [4,34].

XRD studies: The XRD profiles for 0.5; 2.73; 5.07 wt % Cr/SiO_2 samples and silica alone after their oxidation in stream of oxygen at 900°C for 2 hours are presented in Fig. 9. The XRD spectrum of silica consists of a broad diffraction band with maximum intensity at $2\theta = 22°$, characteristic of amorphous silica and with a considerable tailing towards higher diffraction angle. For supported Cr/silica samples additional diffraction lines characteristic for crystalline Cr_2O_3 phase were observed. For low loaded 0.5 wt % Cr/SiO_2 sample, lack of crystalline chromia diffraction lines was observed. Although, at such low Cr loading, the amount of the crystalline Cr_2O_3 phase may be below the detection limit of the XRD technique, its significant formation on silica would be limited, taking into account redox interconversion Cr(VI) ↔ Cr(III) (see Table 2). Also the characteristic yellow color of that sample was unaffected by thermal treatment. In conclusion, it can be inferred that CrO_3 is bonded to the silica surface, forming a highly resistant to thermal destabilization surface phase as definite chromates, being a major component up to 2.73 wt % Cr. For higher chromium loading, the unstable CrO_3 undergoes decomposition when temperature is increased, giving finally crystallites of α-Cr_2O_3. The color of these samples changed from yellow towards green one.

XPS studies: XPS study was undertaken to shed the light on the influence of water on stability of surface chromium oxide phase formed under high temperature treatment of sample and determination of chromium oxidation state as well. Measurements were performed for 2.73 wt % Cr/SiO_2 sample, oxidized both in dry and wet stream of oxygen and for 6.5 wt % Cr/SiO_2 in dry oxygen at 600°C for 2 hours and the XPS spectra are shown in Fig. 10. XPS analysis of the catalysts showed two different oxidation state of chromium Cr(VI) and Cr(III) supported on silica surface with binding energy

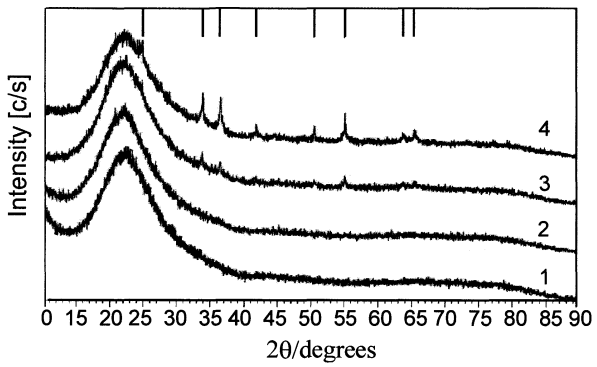

Figure 9. The XRD patterns after calcination in stream of oxygen at 900°C for two hours. Curves: 1 – silica; 2, 3 and 4 for 0.5, 2.73, 5.07 wt % chromium samples, respectively.

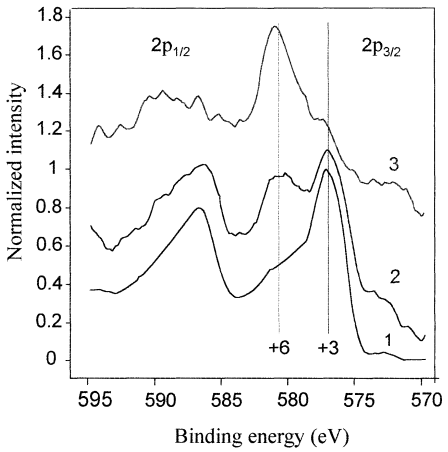

Figure 10. The XPS spectra of CrO_3/SiO_2 samples. Curve 1 refers to the 6.5 wt % Cr/SiO_2 catalyst at calcinated 600°C, 2 h, in dry stream of oxygen. Curves 2 and 3 for 2.73 wt % Cr/SiO_2 catalyst refer to the calcination at 600°C, 2 h, in wet and dry stream of oxygen, respectively

580.7 and 576.9 eV, respectively. The binding energy scale was referenced to BE value 532.8 eV, representing the O 1s peak for the silica support. Our results are in good accordance with literature data: BE Cr $2p_{3/2}$ value for CrO_3 (580.1 eV) and for Cr_2O_3 (576.6 eV) [10]. For lower loaded sample 2.73 wt % Cr/SiO_2 the BE position of $Cr2p_{3/2}$ peaks confirmed the dominant population of chromium(VI) species and relatively small contribution of Cr(III) species stabilized by silica surface (see Fig. 10). On the other hand, chromium(VI) species appeared to be unstable in a stream of wet oxygen under high temperature conditions, leading to partial transformation Cr(VI) $\rightarrow$ Cr(III). Water is involved in the hydrolytic process of monochromates species destabilization, resulting in α-Cr_2O_3 formation. In the case of 6.5 wt % Cr/SiO_2 sample, after high temperature treatment even in a dry oxygen, the XPS spectrum shows the abundance of Cr(III) species. The additional TOF SIMS analysis of Cr/SiO_2 samples showed the most intense chromium clusters for CrO_2, CrO_3, Cr_2O_4, Cr_2O_5 and CrO_3OH, CrOOH fragments, originating from catalyst surface in dry and wet atmosphere, respectively. The crystalline Cr_2O_3 is the most stable among chromium oxides with the enthalpy of formation 180 kcal·mol^{-1}. There is a widely held view that prolonged exposure of the chromium oxides to elevated temperatures, even when on the support surface, results in the increased amount of the highly crystalline phase of α-Cr_2O_3, which may be useless as a catalyst [35,36]. The crystalline α-Cr_2O_3 does not undergo bulk oxidation, but the surface oxidation takes place during the high-temperature oxidation treatment [37]. On the other hand, the formation of a rather a highly mobile and reactive surface Cr(VI) oxo-species has been proposed during the high-temperature oxidation treatment [12,38–40]. They are able to migrate on the silica surface, simultaneously anchoring at the thermodynamically most favorable silica adsorption sites. Chromium trioxide CrO_3 alone is not a stable compound and can be irreversibly decomposed to crystalline α-Cr_2O_3 above 300°C even in oxygen atmosphere, according to:

$$2CrO_3 \rightarrow \alpha\text{-}Cr_2O_3 + 1.5\ O_2 \quad (4)$$

Chromium trioxide CrO_3 supported on SiO_2 surface by wetting impregnation method is anchored to silica surface as chromate like structure formed as a result of:

$$H_2CrO_4 + 2OH^- \rightarrow CrO_4^{2-} + 2H_2O \quad (5)$$

Tetrahedral coordination of Cr(VI) on silica surface leads to chromate species consisting of two terminal oxygen atoms and two oxygen atoms forming strong chemical bonds with silica surface. The strength of these oxygen bridges is responsible for thermal stability of $CrO_3 - SiO_2$ system. The process of $CrO_3 \rightarrow \alpha\text{-}Cr_2O_3$ transformation is possible only when Cr–O–Si linkages undergo splitting. The only reasonable agent responsible for this splitting is water, being the unavoidable component of the CrO_3/SiO_2 system. Water molecules can originate from three possible sources: surface hydroxyl groups, water from gas phase and water being the product of CrO_3/SiO_2 reduction in hydrogen (1) and (2). The process of hydrolytic Cr–O–Si linkages destabilization would be the first step in $CrO_3 \rightarrow \alpha\text{-}Cr_2O_3$ transformation. The sintering of monomolecularly dispersed chromate like species, leading to crystalline chromia supported on silica, would be a sequence of following events: hydrolysis of Cr–O–Si bonds, according to the reverse reaction (4), migration of Cr(VI) hydroxo species and their agglomeration, leading to dehydration and reductive decomposition towards crystalline $\alpha\text{-}Cr_2O_3$, according to reaction (3). Depending on the water vapor content, such mechanism would explain both the experimentally observed tendency of Cr oxo species towards reductive transformation to $\alpha\text{-}Cr_2O_3$ and the surface stabilization of CrO_3 as stable chromate-like species. The above mechanism fits well to oxidative or neutral gas atmosphere. The reduction process in hydrogen likely generates low-valence Cr(III) ions on silica surface and then their hydrolytic destabilization and an activated rearrangement to higher coordination states takes place, resulting in sintering of crystalline chromia phase dispersed on silica. Presence of water in the CrO_3–SiO_2 system may serve as an effective manner of the chromium spreading on the silica surface through successive steps in the hydrolysis anchorage mechanism ensuring attainment of thermodynamic equilibrium [2–3]. On the other hand, an excess of water can lead to splitting of the Cr–O–Si linkages forming $\alpha\text{-}Cr_2O_3$. Of course, the surface concentration of the durable either chromate or polychromate species depends on both the origin of silica and the conditions of treatment such as temperature and oxidative or reductive atmosphere containing tracers of vapor water. Depending on the chromium content and the conditions of the catalyst treatment, either the atomically dispersed chromate species for low chromium loading or the bimodal distribution of chromium phase, consisting of surface chromate species and crystalline $\alpha\text{-}Cr_2O_3$ for higher chromium loaded samples, may be finally expected.

CONCLUSIONS

This work has shown the coexistence of three major forms of chromium oxide phase in the CrO_3/SiO_2 system: monomolecularly dispersed chromates strongly bonded to silica surface, relatively inactive stable crystallites of α-chromia and intermediate metastable amorphous aggregates of CrO_3. The relative contribution of each form strongly depends on the chromium content, method of preparation, treatment conditions (temperature, atmosphere and water traces). The anchoring of chromate-like species requires suitable support adsorption sites and their concentration is governed by hydroxyl group population. Thermodynamically favored chromium sintering process chromates $CrO_4^{2-} \rightarrow$ crystalline α-Cr_2O_3 requires water as a destabilization agent for hydrolytic splitting of Cr–O–Si linkages and chromium oxide agglomeration. Temperature depended oxygen – hydrogen cycling strongly influences the relative composition of chromium oxide phase supported on silica.

Acknowledgments

Financial support for this work was provided under research grant Nr 1262/T09/99/16 of the Polish State Committee for Scientific Research.

REFERENCES

1. Thomas C.L., Catalytic Processes and Proven Catalyst, Academic Press, NY, 1970.
2. McDaniel M.P. and Jonson M.M., *J. Catal*., **101**, 446 (1986).
3. Jóźwiak W.K. and Dalla Lana I.G., *J. Chem. Soc., Farad. Trans*., **93**, 2583 (1997).
4. Jóźwiak W.K., Dalla Lana I.G., Przystajko W. and Fiedorow R., in Proceedings, 9th International Congress on Catalysis, Calgary, 1988 (Phillips M.J. and Ternan Eds.), p. 1340. Chem. Institute of Canada, Ottawa, 1988.
5. Ellison A., Overton T.L. and Bencze L., *J. Chem. Soc. Farad. Trans*., **89**, 843 (1993).
6. Prinetto F., Ghiotti G., De Rossi S. and Di Modica G., *Applied Catalysis B: Environmental*, **14**, 225 (1997).
7. Ruddick V.J. and Badyal J.P.S., *J. Phys. Chem. B*, **102**, 2991 (1998).
8. McDaniel M.P., Witt D.R. and Benham E.A., *J. Catal*., **176**, 344 (1998).
9. Bade O.M., Blom R., Dahl I.M., and Karlsson A., *J. Catal*., **173**, 460 (1998).
10. Storaro L., Ganzerla R., Lenarda M., Zanoni R., López A.J., Olivera-Pastor P. and Castellón E.R., *J. Mol. Catal*., **115**, 329 (1997).
11. Petrosius S.C., Drago R.S., Young V.Y. and Grunewald G.C., *J. Am. Chem., Soc*., **115**, 6131 (1993).
12. Cavani F., Koutyrev M., Trifiro F., Bartolini A., Ghisletti D., Iezzi R., Santucci A. and Piero G.D., *J. Catal*., **158**, 236 (1996).
13. Fouad N.E., Knözinger H., Zaki M.I. and Mansour S.A.A., *Z. Phys. Chem*., **171**, 75 (1991).
14. Köhler K., Engweiler J., Viebrock H. and Baiker A., *Langmuir*, **11**, 3423 (1995).
15. Rachman A., Mohamed M.H., Achmed M. and Aitani A.H., *Appl. Catal*., **121**, 203 (1995).
16. Vuurman M.A., Harcastle F.D. and Wachs I.E., *J. Mol. Catal*., **84**, 193 (1993).
17. Zecchina A., Garrone E., Ghiotti G., Morterra C. and Borello E., *J. Phys. Chem*., **79**, 966 (1975).
18. Cimino A.,Cordischi D., De Rossi S., Ferraris G., Gazzoli D., Indovina V., Occhiuzzi M. and Valigi M., *J. Catal*., **127**, 761 (1991).
19. Hardcastle F.D. and Wachs I.E., *J. Mol. Catal*., **46**, 173 (1988).
20. Kim D.S. and Wachs I.E., *J. Catal*., **142**, 166 (1993).

21. Köhler K., Schläpfer C.W., von Zelewsky A., Nickl J., Engweiler J. and Baiker A., *J. Catal*., **143**, 201 (1993).
22. Fouad N.E., *J. Anal. Cal*., **60**, 541 (2000).
23. Hewston T.A. and Chamberland B.L., *J. Magnetism and Magnetic Mater.*, **43**, 89 (1984).
24. Köhler K., Maciejewski M., Scheider H. and Baiker A., *J. Catal*., **157**, 301 (1995).
25. Mc Daniel P., *J. Catal*., **67**, 71 (1981).
26. Hierl G. and Krauss H.L., *Z. anorg. allg. Chem*., **415**, 57 (1975).
27. Vuurman M.A., Wachs I.E., Stufkens D.J. and Oskam A.J., *J. Mol. Catal*., **80**, 209 (1993).
28. Ellison A. and Overton T.L., *J. Mol. Catal*., **90**, 81 (1994).
29. Zaki M.I., Fouad N.E., Bond G.C. and Tachir S.F., *Thermochim. Acta*, **285**, 167 (1996).
30. Bensalem A., Weckhuysen B.M. and Schoonheydt R.A., *J. Phys. Chem*., **101**, 2824 (1997).
31. Lugo H.J. and Lundsford J.H., *J. Catal*., **91**, 155 (1985).
32. Groeneveld C., Wittigen P.P.M.M., Swinnem H.P.M., Wernsen A. and Schuit G.C.A., *J. Catal*., **83**, 346 (1983).
33. Pollukat T.J. and Hoff R.E., *Catal. Rev.-Sci. Eng*., **41**, 389 (1999).
34. Jóźwiak W.K., Dalla Lana I.G. and Fiedorow R., *J. Catal*., **121**, 183 (1990).
35. Chen J.D. and Sheldon R.A., *J. Catal*., **153**, 1 (1995).
36. Welch M.B. and McDaniel M.P., *J. Catal*., **82**, 110 (1983).
37. Zecchina A., Coluccia S., Cerruti L. and Borello E., *J. Phys*., **75**, 2783 (1971).
38. Schneider H., Maciejewski M., Köhler K. Vokaun A. and Baiker A., *J. Catal*., **157**, 312 (1995).
39. Curry-Hyde H.E., Baiker A., Schraml-Marth M. and Vokaun A., *J. Catal*., **133**, 397 (1992).
40. Schraml-Marth M., Vokaun A., Curry-Hyde H.E. and Baiker A., *J. Catal*., **133**, 415 (1992).